Generation of Nonlinear Vortex Precursors

Yue-Yue Chen, Xun-Li Feng, and Chengpu Liu

Phys. Rev. Lett. **117**, 023901 — Published 7 July 2016

DOI: 10.1103/PhysRevLett.117.023901

Generation of Nonlinear Vortex Precursors

Yue-Yue Chen,[1, 2, 3] Xun-Li Feng,[2] and Chengpu Liu[1, *]

[1] *State Key Laboratory of High Field Laser Physics, Shanghai Institute of Optics and Fine Mechanics, Chinese Academy of Sciences, Shanghai 201800, China*
[2] *Department of Physics, Shanghai Normal University, Shanghai 200234, China*
[3] *University of Chinese Academy of Sciences, Beijing 100039, China*

(Date textdate; Received textdate; Revised textdate; Accepted textdate; Published textdate)

We numerically study the propagation of a few-cycle pulse carrying orbital angular momentum (OAM) through a dense atomic system. Nonlinear precursors consisting of high-order vortex harmonics are generated in the transmitted field due to carrier effects associated with ultrafast Bloch oscillation. The nonlinear precursors survive to propagation effects and are well separated with the main pulse, which provides a straightforward way to measure precursors. By the virtue of carrying high-order OAM, the obtained vortex precursors as information carriers have potential applications in optical information and communication fields where controllable loss, large information-carrying capacity and high speed communication are required.

PACS numbers: 42.65.Ky, 42.65.Re, 42.25.Bs, 42.50.Tx, 42.50.Gy

More than one century ago, the concept of optical precursors emerged from the seminal works of Sommerfeld [1] and Brillouin [2] on asymptotic description of ultrawideband dispersive pulse propagation in linear dielectrics. The precursor associated with the abrupt rising wave front travels at the speed of light in vacuum with nearly no attenuation even in highly absorptive medium [3]. Recently, it has been reported that the precursors also exist in nonlinear interactions regime. Palombini *et al.* theoretically studied the effect of a nonlinear medium response on precursor formation using the split-step Fourier method [4]. Ding *et al.* experimentally observed optical precursors in a four-wave mixing process based on a cold-atom gas [5]. The precursor obtained in nonlinear process is composed of high frequency components and generates no absorption response from the medium [5]. Hereafter we specify the precursors induced by nonlinear effects as nonlinear precursors, otherwise linear precursors. The nearly lossless and fast propagation characteristics of precursor suggest that precursor may find applications in optical communication, biological imaging [6] or underwater communications [7]. To observe precursors, considerable theoretical [8–12] and experimental [13–16] studies on optical precursors have been done over years. However, many initial works focused on opaque media with single or multiple Lorentz absorption lines, where the main signal is either absorbed or unable to be well separated from precursors. This provokes controversies about the existence of precursors [7, 17].

On the other hand, light beams can exhibit helical wave fronts [19, 20]. High-order optical vortex beam has many potential applications such as generating multi-dimensional entanglement to support efficient use of communication channels in quantum cryptography [21], and photoexciting atomic levels without the restriction of standard dipolar selection rules [22, 23]. Recently, promising schemes using plasma [24] and gas [25, 27] as mode converters to generate high-order helical beam in the extreme ultraviolet region have been proposed. The high-order vortex harmonics are obtained by transferring the OAM of the fundamental field to harmonics by high-harmonic generation (HHG), instead of imprinting phase singularities directly to short-wavelength radiation. Zhang *et al.* focused on high-order vortex harmonics generation in the reflected field based on relativistic harmonics from the surface of a solid target ($\sim 1\mu$m) [24]. While the effect of propagation to the generated vortex harmonics was not concerned there. Carlos *et al.* theoretically investigated vortex harmonics generation in linear regime, where the nonlinear propagation instabilities [25] that lead to the decay of high-charged vortices were neglected [27]. Without parametric instabilities, the high-charge vortices resilient to linear propagation were obtained. However, whether high-order vortex harmonics can survive to nonlinear propagation is sill an open question. Moreover, all of these schemes require extremely intense ($\sim 10^{14}$W/cm^2) or even relativistic ($\sim 10^{22}$W/cm^2) laser pulses, and the harmonics information is invisible unless the fundamental field is filtered.

In this Letter, we present a scheme to generate nonlinear precursors consisting of high-order vortex harmonics in relatively low energy physics, where the nonlinear propagation effects are considered. A dense two-level atomic medium is used as a mode converter to manipulate the OAM of a few-cycle helical pulse. Interestingly, nonlinear precursors consisting of high-order vortex harmonics appear in the front of the fundamental field. Compared with that obtained in [24, 25, 27], the high-order vortex harmonics existed in the precursors are intrinsically separated from the fundamental mode, spar-

ing the necessity of a filter to observe the harmonics. Moreover, the high-order vortex harmonics in precursors can be resilient to the parametric instabilities in the nonlinear propagation of the fundamental field. Therefore, our proposal generates high-order vortex harmonics with merits of precursors, relaxes the requirement of extremely intense pulse for ionization or plasma generation, and includes nonlinear propagation effects. Using high-order vortex precursors as information carriers in quantum information can favor the realization of high-speed communication, enhance the efficiency of communication channels, and improve the robustness to resonant absorption loss.

A few-cycle Laguerre-Gaussian (LG) laser pulse ($\sim 10^{12}\mathrm{W/cm^2}$) [28] propagates along z in vacuum and is incident on a dense ($\sim 10^{20}\mathrm{cm^{-3}}$) two-level atomic medium at $z_{in} = 5\mu$m. The interaction between two-state dynamic system and twisted vortex beams has been widely investigated in recent years [29]. The two-state dynamic system provides a direct basis for emerging technology (including quantum control [30]) and for future applications to more complex multi-state and multi-electron systems. Assuming the LG pulse is linearly polarized along x and takes the form of $E(t=0,z) = E_{lp}\cos[\omega_p(z-z_0)/c]\,\mathrm{sech}[1.76(z-z_0)/(c\tau_p)]\hat{e}_x$, where ω_p is the carrier frequency, τ_p the full width at half maximum of the pulse intensity envelop, $\hat{e}_x$ the unit vector in x direction. The initial position z_0 is set to be 3μm to avoid the pulse penetrating into the medium at $t = 0$. The amplitude E_{lp} is defined as [31]

$$\begin{aligned} E_{lp}(t\ =\ 0,z) = {} & \frac{E_0}{(1+\tilde{z}^2/z_R^2)^{1/2}}(\frac{r}{a(\tilde{z})})^l L_p^l(\frac{2r^2}{a^2(\tilde{z})}) \\ & \times \exp(-\frac{r^2}{a^2(\tilde{z})})\exp(-\frac{ikr^2\tilde{z}}{2(\tilde{z}^2+z_R^2)})\exp(-il\phi) \\ & \times \exp(i(2p+l+1)\tan^{-1}\frac{\tilde{z}}{z_R}), \end{aligned} \tag{1}$$

where $\tilde{z} = z - z_0$, E_0 is the peak amplitude of the incident pulse, z_R the Rayleigh range, $a(\tilde{z})$ the radius of the beam, L_p^l associated Laguerre polynomial, and the beam waist a_0 is at $z = z_0$. The characteristic helical phase profiles of optical vortices are described by $\exp(-il\phi)$ multipliers, where $l(l = 0, \pm1, \pm2...)$ is the topological charge corresponding to the mode order and ϕ the azimuthal coordinate. The integer p denotes the number of radial nodes in the mode profile. The three-dimensional Maxwell's equations in an isotropic medium take the form

$$\begin{aligned} \frac{\partial \mathbf{H}}{\partial t} &= -\frac{1}{\mu_0}\nabla\times\mathbf{E}, \\ \frac{\partial \mathbf{E}}{\partial t} &= \frac{1}{\epsilon_0}\nabla\times\mathbf{H} - \frac{1}{\epsilon_0}\frac{\partial \mathbf{P}}{\partial t}. \end{aligned} \tag{2}$$

The macroscopic polarization induced by the linearly polarized electric field is $P_x\hat{e}_x$. $P_x = Ndu$ is associate with the off-diagonal density-matrix element $\rho_{12} = (u+iv)/2$, N the density and d the dipole moment. The population inversion between the excited state 2 and the ground state 1 is denoted by $w = \rho_{22} - \rho_{11}$. u, v and w obey the following set of Bloch equations,

$$\begin{aligned} \frac{\partial u}{\partial t} &= -\gamma_2 u - \omega_0 v, \\ \frac{\partial v}{\partial t} &= -\gamma_2 v + \omega_0 u + 2\Omega w, \\ \frac{\partial w}{\partial t} &= -\gamma_1(w - w_0) - 2\Omega v. \end{aligned} \tag{3}$$

Where γ_1, γ_2 are, respectively, the population and polarization relaxation rates, ω_0 the resonant frequency, $\Omega(z,t)$ the Rabi frequency, and w_0 the initial population difference.

The full wave Maxwell-Bloch (MB) equations can be solved by adopting Yee's finite-difference time-domain (FDTD) discretization method [32, 33] for the electromagnetic fields and the predictor-corrector method [34, 45] or the fourth order Runge-Kutta method [36] for the medium variables. The medium is initialized with $u = v = 0, w_0 = -1$. The following parameters are used to integrate the MB equations: $\omega_0 = \omega_p = 2.3\mathrm{fs^{-1}}$, $d = 2\times10^{29}$A s m, $\gamma_1^{-1} = 1\mathrm{ps}, \gamma_2^{-1} = 0.5\mathrm{ps}, \tau_p = 5\mathrm{fs}, a_0 = 7\mu$m, medium length $L = 25\mu$m, $\Omega_0 = 1.408\mathrm{fs^{-1}}$, the corresponding on-axis pulse area is $A(z) = d/\hbar\int_{-\infty}^{\infty}E_0(z,t')dt' = \Omega_0\tau_p\pi/1.76 = 4\pi$ [37]. Defining a collective frequency parameter $\omega_c = Nd^2/\epsilon_0\hbar = 0.1\mathrm{fs^{-1}}$ to present the coupling strength between medium and field. Our simulation region is padded with perfectly matched layers that prevent back reflection from the truncated simulation region.

With the given parameters, the evolutions of a LG_{10} beam at $z_1 = 9$ μm and $z_2 = 30$ μm are obtained, as shown in Fig. 1. The evolution of a LG_{10} beam with two lobes is quite similar to that of two out-of-phase 2π pulses [38]. For the outer rings with less intensity, it takes more retarded time to achieve a complete Rabi flopping than the inner rings. Therefore the more intense inner rings of each lobe propagate more rapidly, resulting in a crescent-shaped pulse in time-radius plane [39], as shown in Fig. 1(a). However, due to transverse effects, such as transient on-resonance self-focusing caused by the diffraction-induced inward flow of energy from the outer rings [40], the crescent-shaped fields are unstable [41, 42]. Each of them evolves into a leading 2π self-induced transparency (SIT) soliton [43] located at lobe-peak, with the outer rings vanished due to severe energy decrease, as shown in Fig. 1(b).

More importantly, a weak pulse consisting of the third harmonic appears in front of the main pulse during the propagation, as indicated by t_1 in Fig. 1(b). To have a clear view of it, only the third harmonic is shown in Figs. 1(c) and 1(d). It can be seen from Fig. 1(c) that the weak

pulse is generated once the incident pulse propagates into the medium, but has not been separate with the main pulse yet. The transverse electric field distribution at t_1 in Fig. 1(e) still shows the LG_{10}-like mode. With the further propagation, the weak pulse runs ahead of the delayed main pulse (Fig. 1(d)) with an average speed $\upsilon = \frac{z_2 - z_1}{t_2 - t_1} = c$, and an LG_{30}-like mode presents in the transverse plane of electric field at t_1 (Fig. 1(f)). The weak pulse appeared in the front of the main pulse is right the nonlinear precursor discussed in the following.

To avoid the complexity induced by transverse effects, a one-dimensional model is used to further investigate the precursors obtained in our system. As shown in Fig. 2(a), the precursors ahead of a 2π pulse are composed of a rapidly oscillating leading pulse and a long tail. The leading pulse and the tail correspond to an isolated bump around $3\omega_0$ and two bumps near the resonant frequency, respectively, as shown in Fig. 2(b). The former is the nonlinear precursor observed in Fig. 1. The later are the conventional Sommerfeld ($\omega_S > \omega_0$) and Brillouin

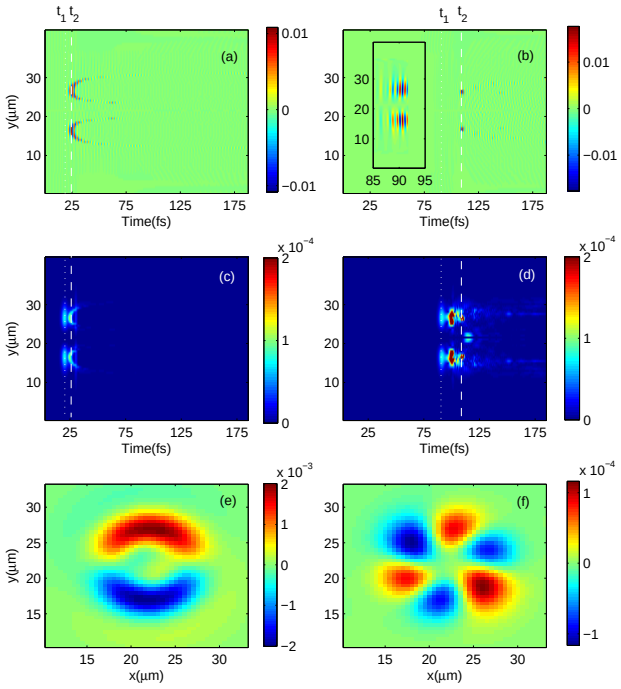

FIG. 1: (color online) Time evolutions of E_x (top) and third harmonic (middle) at z_1 (left) and z_2 (right). (bottom) The corresponding transverse distribution of E_x at t_1. t_1 and t_2 indicate the nonlinear precursor and the main pulse, respectively. The insert in Fig. 1(b) is the enlarged view of the precursors around t_1. For z_1, $t_1 = 20$fs, $t_2 = 24.4$fs; for z_2, $t_1 = 90$fs, $t_2 = 109$fs.

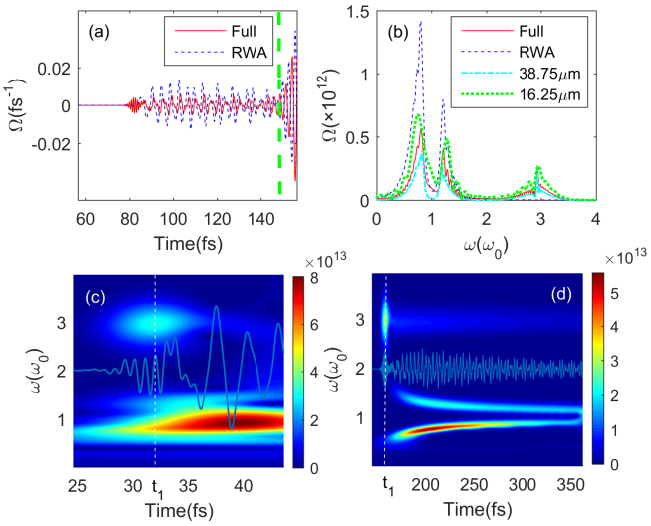

FIG. 2: (color online) The temporal shape of precursors (a) and their spectra (b) at $z = 27.5\mu$m with (solid line) and without (dashed) RWA. The dot-dashed (dotted) line in (b) indicates the spectrum of precursor at $z = 38.75\mu$m ($z = 16.25\mu$m). The time-frequency analysis graphs of precursors at $z = 12.5\mu$m (a) and $z = 50\mu$m (b), respectively. The superimposed solid line shows the corresponding precursor.

($\omega_B < \omega_0$) precursors corresponding to the linear response of a dispersive medium. To explore the origin of the nonlinear precursor, the carrier effects are investigated based on MB equations without RWA. As shown in Fig. 2(a) and 2(b), both the nonlinear precursors and the third harmonic disappear in the framework of RWA. This is because the polarization follows electric field instantaneously and acts as a source of reemitted field. The carrier effects associated with fast oscillation in polarization equations, such as carrier nonlinearity [44] and carrier-wave Rabi flopping (CWRF) [45], are responsible for the generation of harmonics. The carrier effects that are clearly presented in the exact Bloch equations and significant for few-cycle pulses are ignored in the framework of RWA, which leads to the missing of nonlinear precursors. Therefore, the source for nonlinear precursors is the fast oscillations in the Bloch equations beyond the RWA.

Next, let us elaborate the transformation of dominant components of precursors during the propagation. At the beginning of the propagation, the linear precursors are dominant, as shown in Fig. 2(c). As the propagation distance increases, due to the strong on-resonance absorption at high optical depth [46], the spectral bumps in Fig. 2(b) corresponding to Sommerfeld and Brillouin precursors move apart and their spectral amplitudes decrease. In contrast, the nonlinear precursor correspond-

ing to the isolated bump around $3\omega_0$ barely changes as the increase of the propagation depth. This is because, the nonlinear precursor is composed of far-detnuned frequency components and propagates almost losslessly at the speed close to c. Thus, the dominant components of precursors around t_1 change from linear precursors to nonlinear precursors at a large optical depth, as shown in Fig. 2(d). Note that, with the parameters used, the minimal requirement for directly observing the dominant nonlinear precursors is roughly $z > 22.25\mu$m, and larger incident pulse intensity or medium density would relax this requirement.

Based on the above discussion, the nonlinear vortex precursor is expected to be directly observable at a large optical depth, such as $z_2 = 30\mu$m. Indeed, the helical structure of precursors is clearly shown around t_1 in Fig. 3(a). The projection of precursors in $y-t$ plane demonstrates that the distance of rotating one loop of E_x is approximately 0.27μm, which is equal to the wavelength of the third harmonic $\lambda_0/3$ (Fig. 3(c)). The mode of the third harmonic is LG_{30}-like and the changes of the electric field distributions within one loop also show the helical feature (Figs. 3(c)-3(f)). Therefore, the third-order vortex precursor is obtained without the necessity of filtering the fundamental field.

Finally, we give a brief discussion about the influence of parametric instabilities in the nonlinear propagation. During the propagation, the main pulse suffers from azimuthal instabilities and breaks up into spiraling bright spatial solitons [47], which leads to the decay of high-order harmonics in [25]. However, in our scheme higher-order harmonics coexist with the third harmonic in nonlinear precursors. The transverse distributions of

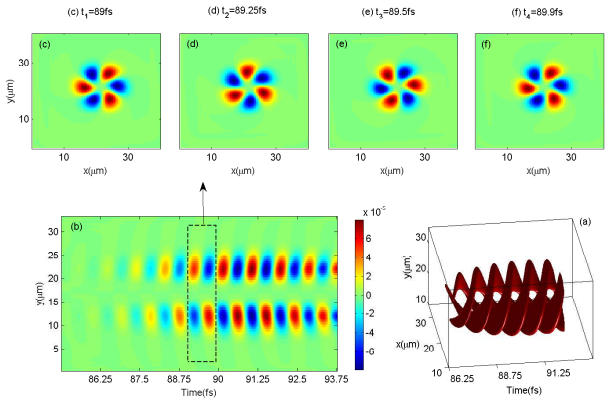

FIG. 3: (color online) (a) The time evolution of E_x at z_2 during [85fs, 93.75fs]. (b) The projection of E_x at $y-t$ plane. (c-f) The distribution of E_x in $x-y$ plane during one rotating loop.

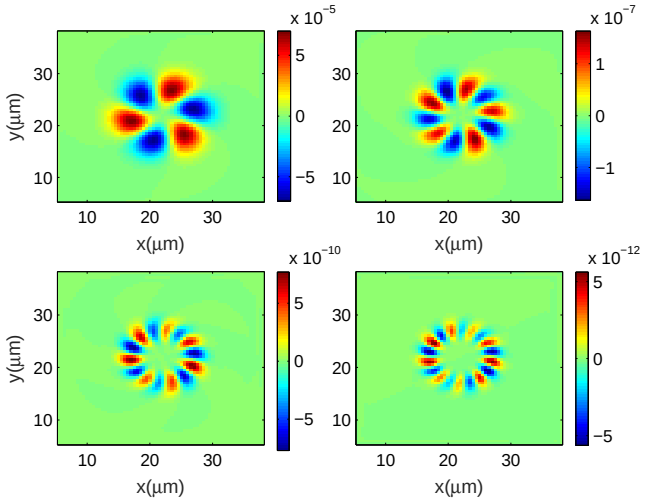

FIG. 4: (color online) Electric field distribution of (a) third, (b) fifth, (c) seventh, and (d) ninth harmonics in $x-y$ plane at t_1 and z_2.

the third, fifth, seventh and ninth harmonics of precursors at z_2 and t_1 are shown in Fig. 4. According to the number of interwind helices, the azimuthal modes of these harmonics are $3, 5, 7, 9$, respectively. The topological charge of the qth-order harmonic is $ql(l = 1)$, which is expected from the HHG theory [26, 27]. Since the intensity of the qth-order harmonic is inversely proportional to q, the transverse structure of precursors is dominated by the LG_{30}-like mode. Thus, even when the parametric instabilities in nonlinear propagation of the fundamental field are present, the high-order vortex harmonics manifested as precursors can still be obtained.

In summary, our scheme provides a way to manipulate the OAM of a beam by means of nonlinear optics without the requirement of extremely intense light. It also combines the merits of both precursors and high-order vortex harmonics. Thanks to the advantage of precursors, the obtained high-order vortex harmonics can propagate at the speed of light in vacuum, and are instinctively separate from the intense fundamental field. They can also survive the parametric instabilities in the nonlinear propagation of the fundamental field and are resilient to absorption. In addition to being information carriers used in high speed communication, precursors can also be used as optical probes of biological tissues or in underwater communication. On the other hand, since the precursors obtained in our scheme consist of high-order vortex harmonics, they have potential applications in quantum information, quantum control and communication where multi-dimensional entanglement is required.

This work is supported by the National Natural Science Foundation of China (NNSF, Grant No.11374318 and No. 11374315) and NSF of Shanghai (Grant No.

15ZR1430600). C.L. is appreciated to the supports from the 100-Talents Project of Chinese Academy of Sciences and Department of Human Resources and Social Security of China.

* Electronic address: chpliu@siom.ac.cn

[1] A. Sommerfeld, Ann. Phys. **44**, 177 (1914).
[2] L. Brillouin, Ann. Phys. **44**, 203 (1914).
[3] S. Zhang, J. F. Chen, C. Liu, M. M. T. Loy, G. K. L. Wong, and S. Du, Phys. Rev. Lett. **106**, 243602 (2011).
[4] C. L. Palombini and K. E. Oughstun, Opt. Express **18**, 23104 (2010).
[5] D-S. Ding, Y. K. Jiang, W. Zhang, Z.-Y. Zhou, B.-S. Shi, and G.-C. Guo, Phys. Rev. Lett. **114**, 093601 (2015).
[6] R. Albanese, J. Penn, and R. Medina, J. Opt. Soc. Am. A **6**, 1441 (1989).
[7] R. R. Alfano, J. L. Birman, X. Ni, M. Alrubaiee, and B. B. Das, Phys. Rev. Lett. **94**, 239401 (2005).
[8] N. A. Cartwright and K. E. Oughstun, SIAM Rev. **49**, 628 (2007).
[9] H. Jeong and U. L. Österberg, Phys. Rev. A **77**, 021803(R) (2008).
[10] H. Jeong and S. Du, Phys. Rev. A **79**, 011802(R) (2009)
[11] B. Macke and B. Segard, Phys. Rev. A **80**, 011803(R) (2009).
[12] W. R. LeFew, S. Venakides, and D. J. Gauthier, Phys. Rev. A **79**, 063842 (2009).
[13] S. Du, P. Kolchin, C. Belthangady, G. Y. Yin, and S. E. Harris, Phys. Rev. Lett. **100**, 183603 (2008).
[14] H. Jeong, A. M. C. Dawes, and D. J. Gauthier, Phys. Rev. Lett. **96**, 143901 (2006).
[15] J. Aaviksoo, J. Kuhl, and K. Ploog, Phys. Rev. A **44**, R5353 (1991).
[16] S.-H. Choi and U. L. Österberg, Phys. Rev. Lett. **92**, 193903 (2004).
[17] U. Österberg, D. Andersson and M. Lisak, Opt. Commun. 277, 5 (2007).
[18] J. E. Rothenberg, Opt. Lett. **17**, 1340 (1992).
[19] A. M. Yao and M. J. Padgett, Adv. Opt. Photonics **3**, 161 (2011).
[20] S. Franke-Arnold, L. Allen, and M. Padgett, Laser Photonics Rev. **2**, 299 (2008).
[21] A. Mair, A. Vaziri, G. Weihs, and A. Zeilinger, Nature (London) **412**, 313 (2001).
[22] A. Afanasev, C. E. Carlson, and A. Mukherjee, Phys. Rev. A **88**, 033841 (2013).
[23] A. Picon, A. Benseny, J. Mompart, J. R. V. de Aldana, L. Plaja, G. F. Calvo, and L. Roso, New J. Phys. **12**, 083053 (2010).
[24] X. Zhang, B. Shen, Y. Shi, X. Wang, L. Zhang, W. Wang, J. Xu, L. Yi, and Z. Xu, Phys. Rev. Lett. **114**, 173901 (2015).
[25] M. Zürch, C. Kern, P. Hansinger, A. Dreischuh, and Ch. Spielmann, Nat. Phys. **8**, 743 (2012).
[26] S. Patchkovskii and M. Spanner, Nat. Phys. **8**, 707 (2012).
[27] C. Hernandez-Garcia, A. Picon, J. San Roman, and L. Plaja, Phys. Rev. Lett. **111**, 083602 (2013).
[28] K. Yamane, Y. Toda, and R. Morita, Opt. Express. **20**, 18986 (2012).
[29] L. Kaplan and J. H. McGuire, Phys.Rev.A **92**,032702 (2015).
[30] P. H. Bucksbaum, Phys. Today **59**, 57 (2006).
[31] L. Allen, M. W. Beijersbergen, R. J. C. Spreeuw, and J. P. Woerdman, Phys. Rev. A **45**, 8185 (1992).
[32] K. S. Yee, IEEE Trans. Antennas Propag. **14**, 302 (1996).
[33] A. Taflove and M.E. Brodwin, IEEE Trans. Microwave Theory Tech. **23**, 623 (1975).
[34] R. W. Ziolkowski, J. M. Arnold, and D. M. Gogny, Phys. Rev. A **52**, 3082 (1995).
[35] S. Hughes, Phys. Rev. Lett. **81**, 3363 (1998).
[36] X.-Y. Xu, W. Liu, and C. Li, Phys. Rev. A **84**, 033811 (2011).
[37] V. P. Kalosha and J. Herrmann, Phys. Rev. Lett. **83**, 544 (1999).
[38] Y. Niu, S. Gong, and N. Cui, J. Korean Phys. Soc. **60**, 1270 (2012).
[39] M. E. Crenshaw and C. D. Cantrell, Phys. Rev. A **39**, 126 (1989).
[40] H. M. Gibbs, B. Bölger, F. P. Mattar, M. C. Newstein, G. Forster, and P. E. Toschek, Phys. Rev. Lett. **37**, 1743 (1976).
[41] Y. Niu, K. Xia, N. Cui, S. Gong, and R. Li, Phys. Rev. A **78**, 063835 (2008).
[42] J. de Lamare, M. Comte, and P. Kupecek, Phys. Rev. A **50**, 3366 (1994).
[43] S. L. McCall and E. L. Hahn, Phys. Rev. 183, 457 (1969).
[44] Y. Xiao, D. N. Maywar, and G. P. Agrawal, Opt. Lett. **38**, 724 (2013).
[45] S. Hughes, Phys. Rev. Lett. **81**, 3363 (1998).
[46] B. Macke and B. Ségard, Phys. Rev. A **86**, 013837 (2012).
[47] W. J. Firth and D. V. Skryabin, Phys. Rev. Lett. **79**, 2450 (1997)